Review **Open Access**

Shuang-yong Xu*

Sequence-specific DNA nicking endonucleases

DOI 10.1515/bmc-2015-0016
Received May 20, 2015; accepted June 24, 2015

Abstract: A group of small HNH nicking endonucleases (NEases) was discovered recently from phage or prophage genomes that nick double-stranded DNA sites ranging from 3 to 5 bp in the presence of Mg^{2+} or Mn^{2+}. The *cosN* site of phage HK97 contains a gp74 nicking site AC↑CGC, which is similar to AC↑CGR (R=A/G) of N.ϕGamma encoded by *Bacillus* phage Gamma. A minimal nicking domain of 76 amino acid residues from N.ϕGamma could be fused to other DNA binding partners to generate chimeric NEases with new specificities. The biological roles of a few small HNH endonucleases (HNHE, gp74 of HK97, gp37 of ϕSLT, ϕ12 HNHE) have been demonstrated in phage and pathogenicity island DNA packaging. Another group of NEases with 3- to 7-bp specificities are either natural components of restriction systems or engineered from type IIS restriction endonucleases. A phage group I intron-encoded HNH homing endonucleases, I-PfoP3I was found to nick DNA sites of 14–16 bp. I-TslI encoded by T7-like ΦI appeared to nick DNA sites with a 9-bp core sequence. DNA nicking and labeling have been applied to optical mapping to aid genome sequence assembly and detection of large insertion/deletion mutations in genomic DNA of cancer cells. Nicking enzyme-mediated amplification reaction has been applied to rapid diagnostic testing of influenza A and B in clinical setting and for construction of DNA-based Boolean logic gates. The clustered regularly interspaced short palindromic repeats-ribonucleoprotein complex consisting of engineered Cas9 nickases in conjunction with tracerRNA:crRNA or a single-guide RNA have been successfully used in genome modifications.

Keywords: DNA nicking endonuclease; DNA optical mapping; genome editing by nickase; nicking enzyme-mediated amplification; strand displacement amplification.

***Corresponding author: Shuang-yong Xu,** New England Biolabs Inc., 240 County Road, Ipswich, MA 01938, USA,
e-mail: xus@neb.com; xus@post.harvard.edu

Introduction

In this article, I will discuss natural DNA nicking endonucleases (NEases or nickases) with 3- to 7-bp specificities, e.g. Nt.CviPII (↓CCD, the down arrow indicates the nicked strand as shown) originally found in chlorella virus (1), engineered NEases such as Nt.BspQI (GCTCTTCN↓), and Nt.BbvCI (CC↓TCAGC) engineered from *Bsp*QI and *Bbv*CI restriction endonucleases (REases) (2, 3). The other group of DNA NEases contains natural or engineered enzymes with more than 8-bp target sites, which includes group I intron-encoded homing endonucleases (HEs) (4, 5), engineered nicking variants from LAGLIDAG HEs (6–8), engineered TALE nucleases (TALENs) by fusion of transcription activator-like effector (TALE) repeat domain with *Fok*I nuclease domain or a *Mut*H nicking variant (9–11), ZF nickase (ZFN) (12–15), RNA-guided Cas9 nicking variants (16, 17), and other chimeric NEases consisting of a DNA binding module fused to a DNA nicking domain (9, 18). Natural NEases related to DNA replication, conjugation, and repair are not covered (19, 20). Readers are encouraged to read recent reviews covering these topics (21, 22).

Naturally occurring HNHE associated with bacterial mobile genetic elements

Small HNHEs associated with phage or prophage

Esherichia coli McrA (Eco_McrA) is an HNH endonuclease (HNHE) encoded by a prophage e14 element that restricted M.HapII-modified plasmid or phage DNA *in vivo* (23, 24). Purified Eco_McrA shows strong binding to 5-methylcytosine (5mCGR, 5mC) in DNA mobility shift assays, but it shows poor methylation-dependent DNA cleavage/nicking activity *in vitro* (25). Another HNHE, gp74 was discovered from *E. coli* phage HK97 that cleaves λ DNA into small fragments in Ni^{2+} or Zn^{2+} buffer (26, 27). Gp74 was shown to be associated with HK97 terminase

large and small subunits (TerL/S) complex and stimulated cleavage/nicking at the cohesive end site (*cos*) (28). It was speculated that TerL-S enzyme may cleave one strand and gp74 may nick the opposite strand. It was convincingly demonstrated that gp74 was involved in DNA packaging and morphogenesis since HK97 gp74 amber mutant (*74am*) produced only empty prohead, but generated normal tails structures that can complement tail-deficient mutants. Furthermore, gp74 amber phage can be rescued by *in vivo* complementation when gp74 is provided in *trans* from a plasmid (28). To analyze the cleavage/nicking sites of gp74, we expressed and purified gp74 (see Supplementary Material). Gp74 was used in digestion of pBR322 plasmid in the presence of divalent cations Mg^{2+}, Mn^{2+}, Ni^{2+}, Co^{2+}, or Ca^{2+}. The enzyme is most active in Mn^{2+} and Co^{2+} buffers (4.4-kb DNA digested into fragments <0.5 kb). In Ni^{2+} buffer, gp74 generated a partial digestion in which a visible banding pattern was detected. The enzyme shows less activity in Mg^{2+} buffer, generating linear and nicked circular DNA and a few partially digested/nicked fragments (when nicks are made in both strands close by, the nicked fragments can be collapsed into cleavage products similar to dsDNA cleavage). To find out the exact cleavage/nicking sites, the nicked DNA was purified and subjected to run-off sequencing (supporting data shown in the Supplementary Material). We found gp74 nicking sites in Mg^{2+} and Ca^{2+} buffers with the consensus sequence AY↑BSS (Y=C/T; B=C/T/G; S=G/C; the up arrow indicates the opposite strand is nicked). Run-off sequencing was also carried out on DNA template pre-nicked in Ni^{2+} buffer. The nicking site consensus sequence AY↑NSV (V=A/C/G, not T; N=A/C/G/T) was found in the Ni^{2+} buffer. Compared to the nicking sites in Mg^{2+} and Ca^{2+} buffers, the nicking specificities in Ni^{2+} buffer are more relaxed in all five positions in the recognition sequence. In summary, most of the nicking sites in Ni^{2+} buffer are 1 base different from the cognate nicking sites found in Mg^{2+} and Ca^{2+} buffers. Another star site, AT↑GCT, also 1 nt off from the cognate site, was nicked in Co^{2+} and Mn^{2+} buffers, but was poorly nicked in Ni^{2+} buffer. This result is consistent with more frequent nicking in Mn^{2+} and Co^{2+} buffers as detected products in agarose gel analysis. In other words, gp74 relaxed the fifth base recognition from V (A/C/G) to N (any base) in Mn^{2+} and Co^{2+} buffers. Since the frequently nicked products were collapsed into small fragments in Mn^{2+} and Co^{2+} buffers, the cleavage products appeared as small fragments generated by 'non-specific' endonucleases. Our run-off sequencing data show that gp74 of phage HK97 is a sequence- and strand-specific NEase that displays unique specificities in the presence of different divalent cations. The nicking specificity appears to be correlated with $Ca^{2+}>Mg^{2+}>Ni^{2+}>Mn^{2+}=Co^{2+}$. The biological significance of this flexible specificity is unknown. The entire phage genome sequence of HK97 is known (29) (GenBank accession number NC_002167.1). Inspection of the rightmost 12-bp sequence (5′-ACCGCCGCCAAA-3′) revealed a potential gp74 nicking site, AC↑CGC-N_7, in Mg^{2+} buffer. By this logic, the top-strand nick would be made by the phage TerL subunit in the gp74-TerS-TerL complex. The single-stranded 10-nt 3′ extension of phage HK97 (5′-AC↑CGCCGCCAAA↓-3′) agrees with this prediction (29).

In *E. coli* cells, Mg^{2+} ions are most abundant with estimated 1- to 2-mM concentration (30). Mn^{2+} ions were estimated in the 10-μM range and free Ca^{2+} ions were in the 1-μM range. Phage terminases usually used Mg^{2+} for catalytic activity in DNA packaging systems *in vitro* (31). In a previous work, we found that N.ϕGamma is active in the presence of Mg^{2+}, Mn^{2+}, Ni^{2+}, or Co^{2+} in a buffer containing 50 mM NaCl, 10 mM Tris-HCl, pH 7.5, and 1 mM dithiothreitol (DTT), but N.ϕGamma shows poor nicking activity in Ca^{2+} buffer. N.ϕGamma displays nicking specificity AC↑CGR in Mg^{2+} buffer. The specificities can be relaxed into 3–4 bp with 1–2 base difference from the cognate site AC↑CGR in Mn^{2+} buffer, with excess enzyme in the nicking reactions or in high concentration of glycerol (10%) (15).

A small HNHE involved in pathogenicity island DNA packaging

Staphylococcal pathogenicity islands (SaPIs) are mobile genetic elements that require helper phages for their DNA replication and packaging into infectious phage-like particles. Some SaPIs encode their own TerS for DNA binding specificity and capsid proteins for smaller genomes. One of the recently identified pathogenicity islands is SaPIbov5 whose genome contains both *pac* and *cos* sites and can be mobilized by two different types of helper phages: one utilizing the *pac* site for headful packaging and terminated by nonspecific cleavage and the second using *cos* site for initiation and termination of DNA packaging (32). Induction, packaging, and mobilization of SaPIbov5 genome by helper phages ϕ12 and ϕSLT are enabled by DNA packaging enzyme TerS-TerL. In addition, a small HNHE (e.g. gp37 of ϕSLT and HNHE of ϕ12) is absolutely required for *cos* site cleavage and packaging. Deletion of the small HNHE genes resulted in a drop of phage titer of 10^5- to 10^6-fold in ϕSLT and ϕ12 infection of natural hosts and a drop of SaPIs packaging efficiency by 10^3- to 10^5-fold. It is speculated that *cos* site cleavage in these helper phages involves the nicking of one strand by TerL/TerS (ATP-dependent endonuclease) and the other

strand by the small HNHEs (32). The precise nicking position by the HNHE at the *cos* site of SaPIbov5 is not determined yet. A structure model of ϕSLT HNHE constructed by homology modeling shows similarity to Gme HNHE that may be involved in DNA repair function (nicking of damaged DNA with AP sites) (33) and to *Pac*I REase found in *Pseudomonas alcaligenes* (34).

More than 20% of long-tailed phage genomes encode an HNHE within five open reading frames (ORFs) of the gene encoding the TerL subunit (15, 28, 32). These *cos* site and terminase-associated HNHEs are almost exclusively found in the Pfam Terminase_1 family, suggesting a conserved biological function in phage DNA packaging or pathogenicity island DNA mobility (28, 32). Tables 1 and 2 show some functional HNHEs associated with phage terminase.

In λ DNA packaging, a specific DNA sequence *cosQ* is required for nicking the bottom strand at *cosN* to generate the 12-nt cohesive end. The top-strand nicking at *cosN* is mostly affected by *cosB* (for TerS subunit-gpNu1 binding) and I2 (for IHF binding), although top-strand nicking is also stimulated by the presence of *cosQ* (35); no HNH NEase is involved in *cosN* cleavage in the initiation or termination of λ DNA packaging. By this logic, it is predicted that ~20% of the long-tailed phage genomes that encode a small HNHE for bottom-strand nicking may not have a functional *cosQ* site for terminase binding to assist nicking of the bottom strand. To initiate DNA packaging, λ terminase complex (gpNu1-gpA) binds to the portal protein of the prohead and nick the *cosN* site of concatemers to translocate DNA into the prohead by ATP-driven reactions. It is speculated that the terminase complex binding to *cosB* that makes the top-strand nick also interacts with the portal vertex and its position is not optimally oriented to nick the bottom strand, thus requiring another terminase complex bound to the *cosQ* site to nick the bottom strand (31, 35).

N.Bis30, N.ϕGamma, and other phage or prophage-encoded HNHE

The HNHEs encoded by phage or prophage are small proteins with 121- to 264-amino acid (aa) residues (Tables 1 and 2) (Figure 1A). The HNHE genes are located adjacent to *terS* and *terL* genes (in some cases, the *terS* gene may be missing) (32). In some phage or prophage genomes, a small gene coding for a zinc ribbon protein co-localized with the HNHE, which may function as a transcriptional regulator (15). The RinA protein (*rinA* gene located upstream of the small *hnh* endonuclease gene) regulates the small HNHE expression level in ϕSLT and ϕ12 (32). We partially purified an HNHE (N.Bis30) encoded by a prophage in the genome of *Bacillus subtilis* T30 (36) (Figure 1A). The nicking sites AC↑CV (V=A/C/G) were determined by run-off sequencing of nicked pBR322 DNA (Figure 1B,C). Figure 1D shows the aa sequence of N.ϕGamma (127 aa) encoded by *Bacillus* phage γ. Serial deletion analysis from the N-terminus demonstrated that

Table 1: Summary of DNA nicking sites by phage- or prophage-encoded HNH NEases.

Phage/prophage HNHE	No. of aa	Nicking site in Mg^{2+} buffer	Nicking site in Mn^{2+} buffer
B. cereus ATCC 10978 (N.BceSVIII)	121	ND (low activity)	S↓RT (AY↑S)
Bacillus phage γ (N.ϕGamma)	127	YCG↓GT (AC↑CGR)	1–2 bp mismatches to YCG↓GT
Bacillus phage 105 (N.ϕ105)	130	YG↓GTY (RAC↑CR)	ND
B. subtilis T30 (N.Bis30)	124	BG↓GT (AC↑CV)	ND
Bacillus thuringensis str T13001 (N.BthT13001)	193	CSG↓GT (AC↑CSG)?	SG↓GT (AC↑CS)
Clostridium phage phi3626 (N.ϕ3626)	142	BCG↓AY (RT↑CGV)	ND
Geobacillus virus E2 (N.ϕE2)	130	CG↓GT (AC↑CG)	ND
Lactobacillus phage Sal2 (N.ϕSal2)	176	WNHTG↓CTC (GAG↑CADNW)?	TG↓CTC (GAG↑CA) or 1–2 bp mismatches
Lactobacillus phage Lrm1 (N.ϕLrm1)	264	ND (low activity)	HSSG↓GT (AC↑CSSD)
S. aureus Y74T prophage Sap040a_009 (N.SauY74I)	119	ND (low activity)	CG↓GT,GG↓GT,TG↓GT,CG↓AT,CG↓GA
Staphylococcus ϕSLT/p37	104	ND	ND
HK97/gp74	119	SSV↓RT (AY↑BSS)	1 bp mismatch to SSN↓RT (AY↑NSS)

ND, not determined; ?, need more experimental evidence; DNA single-letter codes: W, A/T; S, G/C; R, A/G; Y, C/T; B, C/G/T (not A); D, A/G/T (not C); V, A/C/G (not T); H, A/C/T (not G).

Underlined target sites with 4-bp variations (ACCG, ACCR, ACCV, ACCS, RTCG, AGCA, ACYG, and AYBS) are shared by these HNHEs.

Proposed nomenclature: HNH NEase encoded by phage: N.ϕ+phage name, e.g. N.ϕGamma.

Table 2: Genes (ORFs) in proximity to the phage- or prophage-encoded HNH NEases.

Phage or prophage	ZR protein[a]	HNHE	ZR protein[a]	Terminase S[b]	Terminase L	Portal protein
B. cereus ATCC 10978	–	Bce_0389	–	Bce_0390	_0397	_0398
Bacillus phage γ	γLSU_0048	γLSU_0050	–	γLSU_0001	_0002	_0003
Bacillus phage 105	–	phi105_00255	phi105_00260	phi105_00005	_00010	_00020
B. subtilis T30	–	Bis30_20225	Bis30_20220	Bis30_20215	Bis30_20210	Bis30_20200
B. thuringensis str T13001 (Bth193)	–	Bth0005_4180[c]	Unknown			
B. thuringensis str T13001 (Bth67)	Bth0005_53510	Bth0005_53520	–	Bth0005_53530	_53540	Unknown
Clostridium phage phi3626	phi3626_p49	phi3626_p50	–	phi3626_p01	_p02	_p03
E. coli phage ϕP27		p34		p35	p36	p38
E. coli phage ϕHK97		gp74		gp1	gp2	gp3
Geobacillus virus E2	GBVE2_gp069	GBVE2_gp070	–	GBVE2_gp001	_gp002	_gp003
Lactobacillus phage Sal2	–	LSL_279	–	LSL_280	_281	_282
Lactobacillus phage Lrm1	Lrm1_gp52	Lrm1_gp54	–	Lrm1_gp01	_gp02	_gp03
Staphylococcus aureus Y74T (prophage Sap040A)	–	Sap040A_009	Sap040A_010	Sap040A_0011	_012	_014
Staphylococcus ϕSLT		p37		p38	p39	p40

[a]The zinc ribbon motifs of the ZR proteins located either upstream or downstream of the HNHEs contain the aa sequence: CxxC, CxxxC, HxxC, HxxxC, or CxxxxxH.

[b]Terminase small subunits found in Siphoviridae with non-contractile long tails: phage Terminase_4 family, COG3747.

[c]There are two HNHEs in the shotgun genome sequences of *B. thuringensis* str T13001. The N.BthT13001I activity has been verified. The nicking activity of the shorter HNHE (67 aa) and the 110-aa ZR protein is unknown.

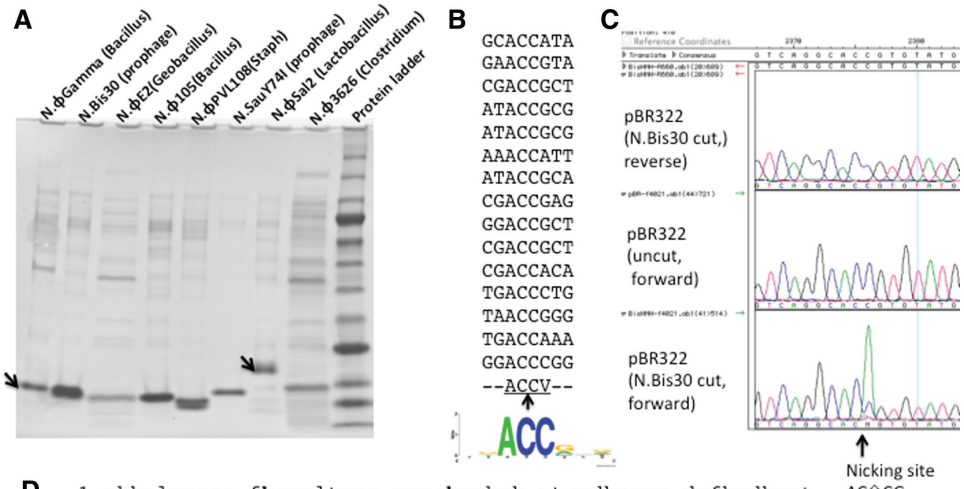

Figure 1: SDS-PAGE analysis of HNHEs, mapping of nicking sites for N.Bis30, and aa deletion analysis of N.ϕGamma.
(A) Example of a few partially purified small HNH NEases. The source of phage or prophage is shown on top of the lanes. (B) N.Bis30 nicking sites in pBR322 as determined by run-off sequencing and compiled by WebLogo (http://weblogo.berkeley.edu/logo.cgi).
(C) Run-off sequencing of one nicking site (ACCG) by N.Bis30. (D) The aa sequence of N.ϕGamma from *Bacillus* phage ϕGamma and a list of four deletion variants to define the minimal active nicking domain. The aa sequence shown in blue is the minimal DNA nicking domain. The important catalytic residues (DH-N-H) are shown in red.

[1] the N-terminal 22 aa could be deleted without significantly affecting the nicking activity in Mg^{2+} and Mn^{2+} buffers; [2] the first 51-aa residues were not absolutely required for the nicking activity in Mn^{2+} buffer, but the truncation mutant (76-aa peptide) displayed impaired nicking activity in Mg^{2+} buffer (the nicking activity can be restored by fusion with a strong DNA binding element such as a zinc finger protein); [3] larger N-terminal deletion, i.e. deletion of 54- or 66-aa residues from the N-terminus completely inactivated the enzyme activity in Mg^{2+} or Mn^{2+} buffer. The minimal HNHE nicking domain of 74- to 76-aa peptide contains a predicted α-helix followed by a typical ββα-metal structure conserved in other HNHEs (15, 18) (Figure 2A,B). The structure prediction (Phyre2 server) (37) of this group of small HNHEs indicates that they are similar to a dimeric Gme_HNH enzyme that prefers to nick damaged DNA (32, 33). The ββα-metal structure is also found in Sra-HNHEs Sco5333 and Tbis1 that display weak non-specific DNA nicking activity in the presence of divalent cations Mg^{2+}, Mn^{2+}, Ni^{2+}, or Co^{2+} (38, 39). Re-assortment of the N-terminus zinc ribbon domain and the C-terminus HNH nicking domain among the HNHEs can also potentially generate new nicking specificities (15).

Natural NEases with 3- to 6-bp specificities

Figure 3 shows a timeline of discovery of naturally occurring and engineered NEases and their applications in research and molecular diagnostics. Nt.CviPII (↓CCD) and Nt.CviQII (R↓AG) are natural DNA NEases originally discovered in chlorella virus-infected lysates (1, 40) and later cloned and expressed in *E. coli* (severe toxicity of Nt.CviQII was encountered when attempting to over-express this enzyme in *E. coli* even in co-expression of M.CviQII) (41, 42). Owing to the frequent nicking sites, the virus genomes carry cognate methylases to modify DNA for self-protection. Nt.BstNBI (GAGTCN4↓), Nt.BspD6I (GAGTCN4↓), Nb.BsrDI (GCAATG↑), Nb.BtsI (GCAGTG↑) are large subunits of the corresponding REases *Bst*NBI, *Bsp*D6I, *Bsr*DI, and *Bts*I (43–46). Nt.BstNBI and Nt.BspD6I are nearly identical isoschizomers with only a 1-aa difference. The small subunit of the *Bsp*D6I is required for bottom-strand cleavage, but it has no DNA binding activity or nuclease activity by itself. The crystal structures of Nt.BspD6I (large subunit) and *Bsp*D6I small subunit have been solved at high resolution, which revealed that Nt.BspD6I contains an N-terminal DNA binding domain, a linker domain, and a

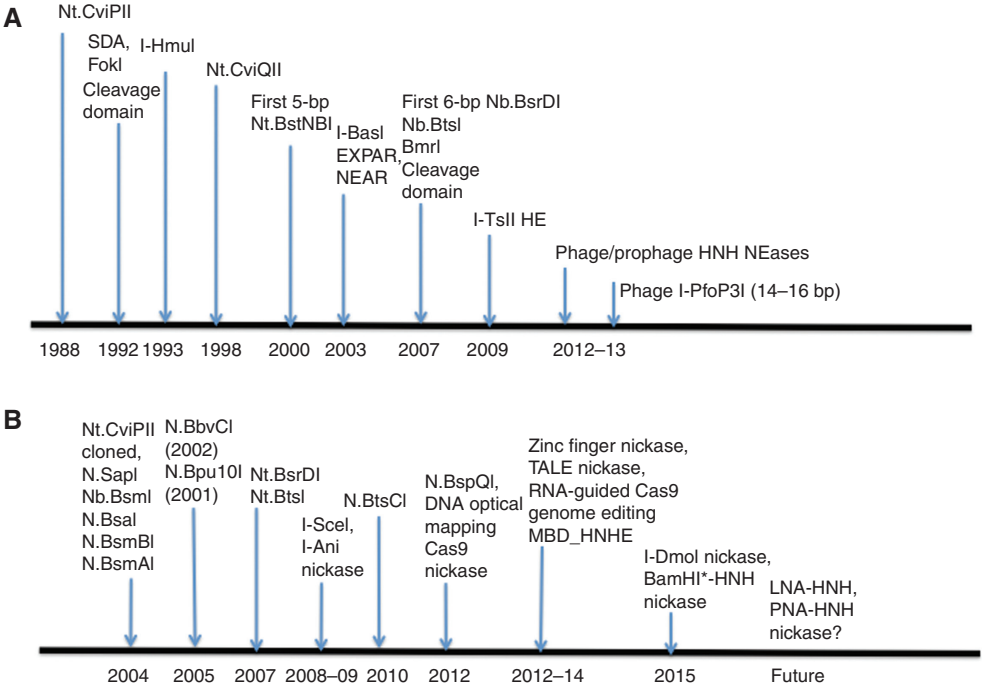

Figure 2: A timeline of nicking enzyme and nuclease cleavage domain (from type IIS REase) discovery (A), engineering (B), and two important NEase applications (EXPAR/NEAR, DNA optical mapping using nicking site profile).
The timeline is not drawn to scale. The timeline is based on the year of publication or issued patent (not based on the time of manuscript submission or patent application). Other DNA nicking enzymes involved in DNA replication, repair, and plasmid transfer (conjugation) are not shown here.

Figure 3: The aa sequence alignment of N.ϕGamma and gp74 of phage HK97.
(A) Schematic output of BlastP analysis using N.ϕGamma aa sequence as a query. The conserved HNH nuclease domain is shown in a blue box where the ββα-metal motif is located. (B) The aa sequence alignment of Gme_HNHE, N.ϕGamma, and HK97_gp74 by web server Promals3d (113). Consensus predicted secondary structure symbols: α-helix: h; β-strand: e. Consensus aa symbols are the following: conserved aa are in bold and uppercase letters; aliphatic (I, V, L): l; aromatic (Y, H, W, F): @; hydrophobic (W, F, Y, M, L, I, V, A, C, T, H): h; alcohol (S, T): o; polar residues (D, E, H, K, N, Q, R, S, T): p; tiny (A, G, C, S): t; small (A, G, C, S, V, N, D, T, P): s; bulky residues (E, F, I, K, L, M, Q, R, W, Y): b; positively charged (K, R, H): +; negatively charged (D, E): -; charged (D, E, K, R, H):c. 4 h9d_chainA, Gme_HNHE from *Geobacillus metallireducens* GS-15 (the 15 C-terminal residues were disordered and not resolved in the structure). The arrows indicate the four important catalytic residues (DH-N-N/H), whose function had been confirmed by site-directed mutagenesis in Gme_HNHE and N.φGamma (18, 33).

C-terminal catalytic domain with the PD-D/E-xK catalytic motif constituted by aa residues E418, D456, E469, E482, and an additional His489 residue near the active site (46). The structure of the Nt.BspD6I cleavage domain is similar to that of *Fok*I endonuclease, which shows non-specific endonuclease activity. In this regard, Nt.BspD6I or Nt.BstNBI nuclease domain may be fused to other DNA binding elements to form chimeric endonucleases with new specificities. One advantage of using Nt.BstNBI nuclease domain is its thermostability at 55°C, which may display improved solubility than the *Fok*I cleavage domain. The Nt.BstNBI nuclease domain has been fused to other DNA binding elements for the construction of chimeric nucleases (G. Wilson, unpublished results). The small subunit of *Bsp*D6I shows 27% aa sequence identity to the C-terminus of the large subunit, but by itself, it lacks any nuclease activity. It must form an enzyme complex with the large subunit in the heterodimer and contribute to the nicking of the bottom strand at N6 downstream of the recognition sequence (GAGTC) (47).

Engineered NEases with 3- to 7-bp specificities

Site-directed mutagenesis of the catalytic sites

Nicking enzyme nomenclature and indication of nicking strand follow the previously established convention (48). Catalytic-deficient large subunit (B subunit) of *Bsr*DI and *Bts*I can form enzyme complexes with the respective WT small subunit (A subunit) to form top-strand NEases (44). Nt and Nb.BsrDI are the most thermostable nicking enzymes, and they are active at 65°C. Nt.BsmAI (GTCTCN↓), Nt.BtsCI (GGATGNN↓), Nt.BsaI (GGTCTCN↓), Nt.BsmBI (CGTCTCN↓), Nb.BsmI (GAATC↑G), Nt.Bpu10I (CC↓TNAGC), Nb.Mva1269I (GAATG↑C), Nt.BbvCI (CC↓TCAGC), Nb.BbvCI (CCTCA↑GC), and Nt.BspQI (GCTCTTCN↓) were engineered from their parent REases by site-directed mutagenesis of the predicted catalytic sites (or critical aa residues near the catalytic site) (2, 3, 49–51) [US patents 6,867,028 (2005) and 7,081,358 (2006)].

Another neat way of making a strand-specific nick is the utilization of type III REase cleavage mechanism. *Eco*P15I (CAGCAG N25/27) requires two sites (head to head or tail to tail) for efficient cleavage. However, it can partially nick a single-site plasmid on the top strand (52). This nicking activity was strongly stimulated by the addition of a nuclease-deficient *Eco*P1I (AGACC N25/27). Since the Res subunits of *Eco*P15I and *Eco*P1I share 95% aa sequence identity, the *Eco*P1I mutant (binding-proficient and catalytic-deficient, DNA helicase$^+$/ATPase$^+$) is able to stimulate *Eco*P15I activity when two enzyme complexes translocate and collide on DNA, leading to *Eco*P15I top-strand nicking. The recently solved *Eco*P15I structure should help our understanding of the nicking mechanism by type III Res-Mod enzyme complex (53).

Site-directed mutagenesis of enzyme dimerization interface

Nt.AlwI (GGATCN4↓) was constructed by domain swapping between *Alw*I and Nt.BstNBI (54), i.e. Nt.AlwI contains the N-terminal DNA recognition domain and catalytic residues of *Alw*I and C-terminal domain of Nt.BstNBI. Nt.AlwI exists as a monomer in solution and only nicks the top strand.

Combining defects in two enzyme functions

N.FokI was constructed by mixing two types of *Fok*I variants, one subunit being binding-proficient and catalytic-deficient and the second subunit being catalytic-proficient with impaired binding. Transient dimerization of *Fok*I variants led to DNA nicking downstream of the *Fok*I site (55).

DNA recognition site mutation or cofactor (pH) alteration

In the monomeric *Bcn*I endonuclease, the enzyme is able to accommodate both C:G and G:C bps at the center of its target site 5′-CCSGG-3′. *Bcn*I crystal structure reveals that *Bcn*I employs two symmetrically oriented His residues H77 and H219 that may alter their protonation states according to two different middle bases (C or G). Site-directed mutagenesis of the two His residues generated two nicking variants, H77A and H219Q, that prefer to nick 5′-CCCGG-3′ and 5′-GGGCC-3′, respectively. Major DNA nicking product by H219Q was detected in a short digestion, but longer digestion also generated some dsDNA cleavage products (56). It was also feasible to lower the pH in digestion buffer to force *Bfi*I to nick only the bottom strand in 5′-ACTGGG-3′ (57). The reaction buffer pH may affect the protonation state of the active site residues.

Nicking RNA/DNA duplexes

The structure and biochemical study of a *Helicobacter pylori* protein HP0268 with a MutS-like domain indicated that HP0268 displays non-specific DNA NEase activity and purine-specific RNase activity in the presence of Mg^{2+} and Mn^{2+} ions. It would be interesting to see whether HP0268 protein could efficiently nick DNA/RNA duplex (58). Very few REases can cut DNA/RNA hybrids: only six type IIP REases (*Ava*II, *Avr*II, *Ban*I, *Hae*III, *Hin*fI, and *Taq*I) are capable of cleaving both DNA and RNA strands in the hybrid duplex (59). Some group II intron-encoded reverse transcriptase enzymes contain an HNHE domain at the C-terminus, which is involved in nicking the DNA site for second-strand cDNA synthesis in the retrohoming process (60, 61).

In summary, more NEases with 4- to 7-bp nicking specificities can be engineered from existing type IIS or type IIP restriction enzymes by mutagenesis of predicted active sites (or important residues near the active site), by altering the dimerization domain, by temporary ‘freezing’ of one recognition mode (protonation state) of a monomeric enzyme with a single active site, by truncation of a monomeric enzyme with two catalytic sites, by changing pH in restriction buffers, or by providing a trans-activating and cleavage-deficient type III REase to a cleavage-competent relative. In theory, cleavage-deficient and binding-proficient REases variants with 3–8 specificities can be fused to an HNH nicking domain or *Fok*I nuclease domain to target and nick DNA. In addition, 5mC-dependent nicking variants may be engineered from the *Msp*JI family of type IIM enzymes (62). We have isolated *Asp*BHI mutants with reduced ds cleavage activity but retaining DNA nicking activities (R. Nugent and S.-y. Xu, unpublished results).

HEs that nick dsDNA

Only two homing NEases with large recognition sequences were reported since the last review on this topic. The first one is I-TslI, a group I intron-encoded HNH HE by T7-like phage ΦI (63). Interestingly, I-TslI homologue can also be found as free-standing endonuclease in phage genome. The precise boundary of the nicking site (~50 bp) is not clearly defined. Cloning and expression of I-TslI in *E. coli* was problematic due to its toxicity (star activity). A catalytic mutant of His residue in the DH-H motif could be

cloned without any difficulty, suggesting that the toxicity was probably caused by DNA damage (S. H. Chan and S.-y. Xu, unpublished results). We managed to purify a small amount of I-TslI by expression of a fusion protein I-TslI-intein-CBD and then cleaving off the tag by intein/DTT cleavage. The partially purified I-TslI appears to nick DNA sites in λ and pBAC plasmid with a 9-bp core sequence 5′-WSCATG↑ATG-3′ (W=A/T), with a few degenerate base recognition downstream of 3′ sequence (R. Nugent and S.-y. Xu, unpublished results). A second HNH homing NEase (I-PfoP3I) was also encoded by a group I intron of phage Pf-WMP3. By serial deletion analysis, the minimal target sequence required for efficient nicking was mapped to a region of 14–16 bp (5′-A↓GCCTAACATCCAACA-3′) (64). Interestingly, I-PfoP3I can utilize Mg^{2+}, Mn^{2+}, and Ca^{2+} for nicking activity. A second nicking site of I-PfoP3I was mapped in a DNA polymerase gene of Pf-WMP4 (predicted intron homing site) that contains a related recognition sequence of 5′-C↓CCCCAACATGCAGAA-3′ (the precise boundary is not clearly defined in this site). The intron homing sites of DNA polymerase genes of phage Bastille, SPO1, and SPO2 are also similar, but the corresponding homing NEases I-HmuI and I-BasI nick the opposite strand at a different position (5). It remains to be seen whether I-PfoP3I with 16-bp nicking sites could be used in DNA optical mapping (an equivalent of ~13-bp specificity if the degenerate positions are accounted for in two nicking sites 5′-M↓SCCYAACATSCARMA-3′) (M=A/C, R=A/G, S=G/C). Three nickases have been engineered from their corresponding LAGLIDADG HEs: I-SceI, I-AniI, and I-DmoI (6–8), but the best nicking mutant engineered from I-DmoI still displays significant amounts of dsDNA cleavage, and further optimization may be necessary for *in vivo* application (8). Overall, the nicking variants are less toxic and caused much lower insertion/deletion mutations in gene editing applications [since DNA nicks are repaired by homology-directed repair (HDR), not by non-homologous end joining (NHEJ)] (65–67). These studies were the first ones to analyze and compare the repaired end products by site-directed nicks and dsDNA breaks.

Engineering of chimeric NEase using the 76-aa nicking domain of N.ϕGamma

The 76-aa nicking domain of N.ϕGamma has been fused to zinc finger protein Zif268 and 5mCpG binding domain of MBD2 to create chimeric nicking enzymes. A 13-aa linker was introduced to connect the Zif268 and the 76-aa nicking domain. The fusion enzyme prefers to nick a composite site 5′-AT↑CGN$_6$ GCGTGGGCG-3′ (underlined sequence=Zif268 binding site) (15). When the 76-aa nicking domain was fused to the duplicated 5mCpG-binding domain of MBD2, the chimeric nicking enzyme can be targeted to 5mCpG sites in a high-salt buffer (0.2–0.3 M KCl). However, the nicking distance is variable (5′-AC↑YGG N$_{8–15}$ 5mCpG-3′), probably conferred by the duplicated 5mCpG-binding domain (18). Recently, we fused a 76-aa nicking domain (an attenuated double mutant) to a binding-proficient and cleavage-deficient *Bam*HI mutant (D94N/E113K) (68). The chimeric enzyme prefers to nick a composite site 5′-GGATCC-N$_{(4–6)}$-AC↑CGX-3′ (X: G>A>C=T) in high-salt buffers. The chimeric nicking enzyme also nicks a symmetric site CCG↓GT-N$_5$-GGATCC-N$_5$-AC↑CGG, creating a 20-nt overhang after nicking (S.-y. Xu, unpublished result). There are over 400 unique type II REase specificities (69). A large number of cleavage-deficient REases have been isolated before (e.g. *Eco*O109I, *Eco*RI, *Eco*RV, *Bso*BI, *Bsp*QI, *Hin*cII, *Not*I, *Pac*I, *Pvu*II, and *Ppu*MI). The cleavage-deficient and binding-proficient variants of REases (4–8 bp) can be coupled with the 76-aa nicking domain to generate NEases with 8.5- to 12.5-bp nicking specificities, which fill in the gap between natural NEases (3–6 bp) and HE NEases with >16-bp target sites.

Applications in genome modifications (gene editing: insertion, deletion, correction)

With engineered HE nicking enzymes

Enzyme engineering can be applied to generate superior enzyme variants with stringent specificities that can perform complete nicking of target sites. Other HEs with dsDNA cleavage activity with relative short recognition sequence can also be engineered to nick just one strand. In gene targeting experiments using an engineered I-AniI nicking variant, the ssDNA nick efficiently induces homology-directed recombination (HDR) with plasmid or adeno-associated virus vector templates. The severe toxicity by the parent dsDNA cleavage enzyme was reduced to a minimal level when the nicking variant was co-expressed in transfection assays. In a separate study, the I-SceI nicking variant (K223I) was shown to stimulate gene correction efficiency up to 12-fold in yeast and human cells *via* homologous recombination with a template DNA (67). A large number of putative HNH HEs remain to be characterized from sequenced genomes. For example, the genome of chlorella virus NY-2A contains 18 predicted HNH HEs with unknown specificities (J. Van Etten, unpublished results). In the non-tailed genomes of

brucellaphages, there is a conserved HNHE encoded by intein that is inserted out of frame in the large subunit of terminase gene (70). The HNHE is thought to play a role in intein mobility. It is not clear whether this HNHE is a nicking enzyme or a dsDNA cutter.

With DNA binding domain nuclease (nicking) domain fusions (zinc finger nickase and TALE nickase)

The *Fok*I endonuclease catalytic residues were identified in early 1990s (71), and its crystal structure in complex with DNA was solved in high resolution (72). Trypsin digestion and mapping of *Fok*I endonuclease indicated that a 25-kDa C-terminal domain is a non-specific endonuclease (73) that could be fused to a zinc finger protein to generate chimeric endonuclease known as ZFN (74). Since *Fok*I cleavage requires transient dimerization of two cleavage domains (75), ZF nickase consisted of ZFN1 fused to WT-*Fok*I cleavage domain and ZFN2 fused to a catalytic-deficient *Fok*I nuclease domain (D450A or D467A) that can be engineered to nick the target site on one strand. Joung and coworkers reported that ZFN nickases generated reduced off-target mutations in comparison with dsDNA cutter ZFN (14), as DNA nicks are repaired by HDR that reduces the unwanted off-target insertion/deletion generated by NHEJ repair pathway from dsDNA breaks. The use of TALE nickases in genome editing has also been reported to modify human and animal genomes with remarkable success (10, 11). In general, the gene editing efficiency from a single nick is 1–2 orders of magnitude lower than that caused by dsDNA breaks (9–14). To increase gene-editing efficiency, two pairs of ZFN nickase or TALEN nickase can be used to generate nicks on both strands, and this double-nicking strategy may increase target specificity and gene-targeting efficiency and minimizes off-target mutations. The knowledge researchers accumulated from study of REase-derived nicking enzymes, HE nicking variants, ZFN, and TALEN nickases helped scientists to optimize a new gene targeting technology (see below).

With nicking enzymes guided by RNA

The clustered regularly interspaced short palindromic repeats (CRISPR)-Cas-adaptive immune systems in bacteria and archaea target foreign nucleic acids (e.g. viral DNA or RNA) for degradation [reviewed in (76)]. The Cas9 endonuclease from type II CRISPR-Cas systems utilizes two small RNA molecules, tracerRNA and crRNA, to target and cleave invading viral DNA. The crRNA was processed by RNaseIII and unknown nuclease(s) from pre-CRISPR RNA transcripts that transcribed from CRISPR arrays (the short foreign DNA fragments known as protospacer were acquired and inserted into the CRISPR array as 'memory' elements during previous unsuccessful infections). The tracerRNA and crRNA can be fused together to form a single guide RNA to direct Cas9 endonuclease to target DNA provided that a short DNA sequence known as protospacer adjacent motif (PAM) is present in the (-) strand (a '-' strand is defined as the non-complementary strand to crRNA; '+' strand is complementary to crRNA). Each Cas9 protein has evolved to preferentially recognize its own PAM motif (specificity). However, up to five mismatches out of 20–22 nt are tolerated in the sgRNA sequence, potentially generating many unintended mutations by Cas9-sgRNA-mediated gene modification (16, 77). To overcome this deficiency, Cas9 nicking variants have been engineered by mutating one of the two catalytic sites analogous to engineering of N.BbvCI and N.BtsCI. The Cas9 protein of *Streptococcus pyogenes* carries two putative catalytic motifs, one RuvCI-like catalytic motif (RuvC motif I) located at the N-terminus and an HNH (HNN) catalytic motif located in the middle of the protein. Cas9-D10A variant makes a specific nick in the complementary strand (+), and the Cas9-H840A variant gave rise to multiple nicked products (3–4 bands) in the non-complementary strand (-), possibly trimmed by the 3′-5′ exonuclease activity of Cas9 (16). The exonuclease degradation of the target DNA may provide an advantage to the host surveillance system since the ends are not easily repaired by a simple ligation step in bacteria. Similarly, the Cas9 protein from *Streptococcus thermophilus* DGCC7710 was also mutated to generate (+) strand nicking variant D31A and (-) strand nicking variant N891A (17). Ten to 30 min of digestion of the (-) strand by Cas9-N891A also generated multiple cleavage products, suggesting further processing by the 3′-5′ exonuclease activity of the mutant enzyme. The Cas9 endonucleases cleave target DNA 3-nt upstream of the PAM sequence to generate blunt ends, which may be further degraded by host exonucleases (16). Since the successful creation of Cas9 nicking variants, double nicking by sgRNA-Cas9n have been used in multiple genome targeting experiments to reduce off-target mutations and at the same time enhance gene editing efficiency and specificity (76, 78–81). RNA-guided Cas9 nickases have been successfully used in other genome modification experiments in bacterial cells (82), plant cells (83, 84), *Drosophila* cells (85), mouse cells and embryos, and human cells (79, 86–91). Using a nickase variant of Cas9 and simultaneous introduction of two guide RNAs that recognize adjacent targets are necessary to make a double-strand break. As a result, the

frequency of undesired off-target DSBs is greatly reduced using a Cas9 nickase with two guide RNAs, as compared to wild-type Cas9 with only one guide RNA.

In theory, Cas9 nickases can be used for gene cloning following nicking of two DNA strands and insert ligation with two non-complementary ends or vector-insert assembly by Gibson method. A 22-kb bluntly cut vector by Cas9 and sgRNA was successfully used for cloning of a DNA fragment (92). It will be interesting to see whether sgRNA-Cas9 nickases can be programmed to cut single-stranded RNAs by RNA interference (RNAi). It has been shown that Cas9 endonuclease from *Francisella novicida* (FnCas9) in complex with sgRNA can be used to target (+) strand ss-viral RNA and hepatitis C virus RNA and inhibit viral replication (93). *Thermus thermopilus* type III-B CRISPR-Cas systems exclusively target ssRNA for degradation and not DNA sequences that are complementary to the crRNA [reviewed in (76)]. Smaller SaCas9 protein (~1 kb shorter *sacas9* gene coding sequence) and nicking variants encoded by a *Staphylococcus aureus* strain have been found in sequenced bacterial genomes and cloned into an adeno-associated virus vector with sgRNA coding sequence for genome modification in a mouse model (94).

DNA optical mapping

Nt.BspQI was applied to nicking site profiling in a proof-of-concept experiment on a phage DNA (2). DNA optical mapping was applied to bacterial artificial chromosome (BAC) clones containing large human DNA inserts for *de novo* sequence assembly and for detection of structural variations in complex regions (95). Nt.BspQI and Nt.BbvCI have been used in nicking and labeling of BAC clones of the complex genome of *Aegilops tauschii* with two different fluorophores. The nicking site map derived from nanochannel arrays facilitated the correct contigs assembly of *de novo* genome sequences. The nicking site-guided assembly improved the accuracy from the initial 75% to 95% completion of the genome sequences (96).

Sequence amplification for diagnostic detection

REase-directed nicking of phosphorothioate-modified DNA

Before strand- and sequence-specific NEases were commercially available, researchers used certain restriction enzymes to nick DNA after incorporation of 5′-dA/dC/dG/dT [α-S]-triphosphate into restriction sites. An initial test of hemi-phosphorothioate-modified restriction sites indicated that [1] the modification needs to be incorporated in the exact cleavage sites; [2] the first group of REases predominantly nicks the unmodified strand, resulting in nicked DNA (i.e. hemi-phosphorothioate-modified strand inhibits cleavage of that strand); [3] the second group of REases slowed down the nicking of the modified strand (nicked circular DNA can still be obtained in limited digestion); [4] the third group of REases cleaves both strands (nicked intermediate was converted to linear DNA before all supercoiled DNA was nicked) (97). In the early 1990s, REase-mediated nicking of hemi-phosphorothioate DNA after incorporation of 5′-deoxyadenosine [α-S]-triphosphate was applied to commercial applications. The nicked template and two primers were used in isothermal (exponential) strand displacement amplification (SDA) when *Hinc*II was used to nick template DNA and a Klenow fragment of *E. coli* DNA polymerase I (5′-3′ exonuclease-deficient) catalyzed strand displacement and primer extension (98, 99). By combination of *Bso*BI and 5′-3′ exonuclease-deficient Bca DNA polymerase (or *Bst* DNA polymerase large fragment) in the presence of hemi-phosphorothioate-modified template DNA, a thermophilic SDA method was further developed (100).

EXPAR and NEAR

The first NEase-mediated isothermal exponential amplification (EXPAR) was reported in 2003 (101). It took more than 10 years of development to commercialize this technology (also termed ‘NEAR’ for nicking enzyme-mediated amplification reactions) in the clinical setting for rapid influenza A and B diagnostics. Because of the fast speed (signal detection in 5–10 min) and no requirement for thermocycling, NEAR has a certain advantage over PCR-based amplification reactions. The disadvantage of using NEAR is the absolute requirement of highly purified DNA polymerase and NEases that have very little nucleic acid contamination. Pre-incubation of *Bst* DNA polymerase large fragment with EXPAR (NEAR) templates significantly increases non-specific background amplification (102). Although NEase is not critical for initiating non-specific amplification, it is required to propagate the reaction once initiated. NEases are also known to create *de novo*, non-template-dependent synthesis of repetitive sequences (103). Nb.BbvCI was used in enzyme-assisted signal amplification in microRNA detection from cell lysates; high sensitivity and selectivity were detected (104). A biosensor for

Ag^{+} detection utilized the Nt.CviPII to nick a ligated probe for electrode regeneration with a detection limit of 0.1 nm of the heavy metal (105).

Nicking enzymes to generate long sticky ends for cloning (fragment assembly)

Nt.BspQI has been used in ligation-independent cloning of PCR products (106, 107). Nt.BbvCI was used to nick a plasmid to generate sticky ends for PCR fragment assembly with USER enzymes (uracil DNA glycosylase and DNA endonuclease VIII), which cleave the PCR primer region with pre-designed uracil (108).

Logic gates

In DNA-based molecular control circuits, controller DNA components are made by synthetic DNA molecules and cloned into plasmid vectors to produce large quantities in *E. coli* cells. Both the input and output signals are short dsDNA sequences that are generated by NEases and strand-displacement amplification carried out by a DNA polymerase in conjunction with a detection DNA oligo reporter with a fluorophore and a quencher. DNA gate production can be carried out by restriction digestion. Nicked dsDNA gates (join gates and fork gates) are generated by treatment with Nb.BsrDI and Nt.BstNBI, respectively (109). The utilization of nucleic acids and protein (enzymes) in the construction of Boolean logic gates was reviewed recently (110). Other molecular diagnostic applications using DNA NEases can be found in the previous review article (111). A review article on isothermal amplification and detection of DNA and RNA *via* NEase signal amplification and NEase-assisted nanoparticle activation was recently published (112).

Expert opinion and outlook

More DNA NEases with 3- to 7-bp specificities will be created in the near future by structure-guided and catalytic site-based mutagenesis or by genome mining of putative heterodimeric REases found in many sequenced microbial genomes. The capability of engineering sequence specificities from type IIS or type IIG REases and solving the enzyme structures will pave the way for creating more 6- to 8-bp nicking specificities. The availability of rare nicking specificities will empower DNA optical mapping and improve the accuracy of *de novo* sequence assembly and detect large insertion/deletion in cancer genomes. NEAR will be applied to more clinical diagnostics owing to its rapid isothermal amplification and detection. RNA-guided Cas9 nicking variants will be applied to plant and human genome editing for crop improvement and for curing genetic diseases. 5mCpG-specific chimeric nicking enzymes may be applied to epigenetic analysis of cancer genomes during anti-cancer drug treatment. N.Bis30 variants will be isolated to nick more relaxed sites such as ACC (WT nicking site, ACCV) in the presence of Mg^{2+}. The small HNH nicking domain will be fused to other DNA binding partners to create nicking specificities of 8–14 bp that fill the gap of frequent NEases and HEs. Future development of invader locked nucleic acid (LNA), helix-invading peptide nucleic acids (PNAs), or pseudo-complementary PNA coupled with a small HNH nicking domain with 2- to 3-bp specificities will facilitate these chimeric NEase applications in genome editing. Engineered heterodimeric *Fok*I or other type IIS cleavage/nicking variants will be coupled to LNAs or PNAs to introduce specific nicks in DNA to facilitate HDR in genome editing. Cas9 nicking variants with multiple mutations will be constructed to eliminate residual dsDNA cleavage. Unintended off-target mutations introduced by gene editing nickases will be minimized in human and animal embryonic stem cells and animal models, and ultimately, gene modification reagents will be put into clinical trials.

Highlights

- The small HNHEs involved in phage DNA packing and pathogenicity island mobility are widespread in nature.
- ϕHK97 gp74 is a sequence- and strand-specific nicking enzyme. It recognizes and nicks DNA sites in Mg^{2+} and Ca^{2+} buffers. Its nicking specificity is more relaxed in Ni^{2+}, Mn^{2+}, and Co^{2+} buffers.
- I-PfoP3I nicks DNA sites of 14–16 bp with degenerate recognition at some positions. I-TslI expression in *E. coli* is extremely toxic and it appears to nick DNA sites with a 9-bp core sequence.
- Natural NEases with 5- to 6-bp specificities are found to be part of heterodimeric REases (large subunits). Frequent nicking natural NEases *Cvi*PII and *Cvi*QII were originally discovered in chlorella virus lysates and the viral genomes also encode cognate MTases for self-protection.
- NEases can be readily engineered from type IIS and type IIP REases by site-directed mutagenesis of catalytic sites, altered dimerization state, domain

swapping, or fixation of a particular recognition mode.
- DNA optical mapping using NEases and fluorescent labeling at the nicked sites and subsequent detection on nanochannel arrays can generate nicking site profiles to aid complex genome assembly and significantly improve the accuracy.
- NEAR has found its way in influenza A and B diagnostics due to its rapid speed and no requirement for thermocycling.
- Paired nicking by RNA-guided CRISPR-Cas9 nickase can enhance genome editing specificity and significantly reduce off-target mutations.

Acknowledgments: I thank Lise Raleigh, William Jack, and Richard Roberts for critical comments; Siu-Hong Chan and Rebecca Nugent for unpublished information; Sonal Gidwani for help with ϕHK97 gp74 purification; Geoff Wilson for helpful discussions; and Barry Stoddard and the anonymous reviewers for helpful suggestions to improve the manuscript. Research in Xu's laboratory was supported by New England Biolabs (NEB), Inc. I thank Don Comb and Jim Ellard for continued support. The open access fee is paid for by NEB.

Conflict of interest statement: Some nicking enzymes mentioned in this article are products of NEB, Inc., where the author is currently employed.

References

1. Xia Y, Morgan R, Schildkraut I, Van Etten JL. A site-specific single strand endonuclease activity induced by NYs-1 virus infection of a chlorella-like green alga. Nucleic Acids Res 1988; 16: 9477–87.
2. Zhang P, Too PH, Samuelson JC, Chan SH, Vincze T, Doucette S, Bäckström S, Potamousis KD, Schramm TM, Forrest D, Schwartz DC, Xu SY. Engineering BspQI nicking enzymes and application of N.BspQI in DNA labeling and production of single-strand DNA. Protein Expr Purif 2010; 69: 226–34.
3. Heiter DF, Lunnen KD, Wilson GG. Site-specific DNA-nicking mutants of the heterodimeric restriction endonuclease R.BbvCI. J Mol Biol 2005; 348: 631–40.
4. Landthaler M, Shub DA. The nicking homing endonuclease I-BasI is encoded by a group I intron in the DNA polymerase gene of the Bacillus thuringiensis phage Bastille. Nucleic Acids Res 2003; 31: 3071–7.
5. Landthaler M, Shen BW, Stoddard BL, Shub DA. I-BasI and I-HmuI: two phage intron-encoded endonucleases with homologous DNA recognition sequences but distinct DNA specificities. J Mol Biol 2006; 358: 1137–51.
6. Niu Y, Tenney K, Li H, Gimble FS. Engineering variants of the I-SceI homing endonuclease with strand-specific and site-specific DNA-nicking activity. J Mol Biol 2008; 382: 188–202.
7. McConnell Smith A, Takeuchi R, Pellenz S, Davis L, Maizels N, Monnat RJ Jr, Stoddard BL. Generation of a nicking enzyme that stimulates site-specific gene conversion from the I-AniI LAGLIDADG homing endonuclease. Proc Natl Acad Sci USA 2009; 106: 5099–104.
8. Molina R, Marcaida MJ, Redondo P, Marenchino M, Duchateau P, D'Abramo M, Montoya G, Prieto J. Engineering a nickase on the homing endonuclease I-DmoI scaffold. J Biol Chem 2015. PII: jbc.M115.658666 [Epub ahead of print].
9. Gabsalilow L, Schierling B, Friedhoff P, Pingoud A, Wende W. Site- and strand-specific nicking of DNA by fusion proteins derived from MutH and I-SceI or TALE repeats. Nucleic Acids Res 2013; 41: e83.
10. Wu Y, Gao T, Wang X, Hu Y, Hu X, Hu Z, Pang J, Li Z, Xue J, Feng M, Wu L, Liang D. TALE nickase mediates high efficient targeted transgene integration at the human multi-copy ribosomal DNA locus. Biochem Biophys Res Commun 2014; 446: 261–6.
11. Wu H, Wang Y, Zhang Y, Yang M, Lv J, Liu J, Zhang Y. TALE nickase-mediated SP110 knockin endows cattle with increased resistance to tuberculosis. Proc Natl Acad Sci USA 2015; 112: E1530–9.
12. Wang J, Friedman G, Doyon Y, Wang NS, Li CJ, Miller JC, Hua KL, Yan JJ, Babiarz JE, Gregory PD, Holmes MC. Targeted gene addition to a predetermined site in the human genome using a ZFN-based nicking enzyme. Genome Res 2012; 22: 1316–26.
13. Kim E, Kim S, Kim DH, Choi BS, Choi IY, Kim JS. Precision genome engineering with programmable DNA-nicking enzymes. Genome Res 2012; 22: 1327–33.
14. Ramirez CL, Certo MT, Mussolino C, Goodwin MJ, Cradick TJ, McCaffrey AP, Cathomen T, Scharenberg AM, Joung JK. Engineered zinc finger nickases induce homology-directed repair with reduced mutagenic effects. Nucleic Acids Res 2012; 40: 5560–8.
15. Xu SY, Gupta YK. Natural zinc ribbon HNH endonucleases and engineered zinc finger nicking endonuclease. Nucleic Acids Res 2013; 41: 378–90.
16. Jinek M, Chylinski K, Fonfara I, Hauer M, Doudna JA, Charpentier E. A programmable dual-RNA-guided DNA endonuclease in adaptive bacterial immunity. Science 2012; 337: 816–21.
17. Gasiunas G, Barrangou R, Horvath P, Siksnys V. Cas9-crRNA ribonucleoprotein complex mediates specific DNA cleavage for adaptive immunity in bacteria. Proc Natl Acad Sci USA 2012; 109: E2579–86.
18. Gutjahr A, Xu SY. Engineering nicking enzymes that preferentially nick 5-methylcytosine-modified DNA. Nucleic Acids Res 2014; 42: e77.
19. Higashitani A, Greenstein D, Hirokawa H, Asano S, Horiuchi K. Multiple DNA conformational changes induced by an initiator protein precede the nicking reaction in a rolling circle replication origin. J Mol Biol 1994; 237: 388–400.
20. Francia MV, Clewell DB, de la Cruz F, Moncalian G. Catalytic domain of plasmid pAD1 relaxase TraX defines a group of relaxases related to restriction endonucleases. Proc Natl Acad Sci USA 2013; 110: 13606–11.
21. Tsutakawa SE, Lafrance-Vanasse J, Tainer JA. The cutting edges in DNA repair, licensing, and fidelity: DNA and RNA repair nucleases sculpt DNA to measure twice, cut once. DNA Repair (Amst) 2014; 19: 95–107.
22. Balakrishnan L, Bambara RA. Flap endonuclease 1. Annu Rev Biochem 2013; 82: 119–38.

23. Raleigh EA, Trimarchi R, Revel H. Genetic and physical mapping of the mcrA (rglA) and mcrB (rglB) 1989; 122: 279–96.
24. Hiom K, Sedgwick SG. Cloning and structural characterization of the mcrA locus of Escherichia coli. J Bacteriol 1991; 173: 7368–73.
25. Mulligan EA, Hatchwell E, McCorkle SR, Dunn JJ. Differential binding of Escherichia coli McrA protein to DNA sequences that contain the dinucleotide m5CpG. Nucleic Acids Res 2010; 386: 1997–2005.
26. Moodley S. Biochemical investigation of the bacteriophage protein HK97 gp74. MS thesis, University of Toronto, 2010: 1–102.
27. Moodley S, Maxwell KL, Kanelis V. The protein gp74 from the bacteriophage HK97 functions as a HNH endonuclease. Protein Sci 2012; 21: 809–18.
28. Kala S, Cumby N, Sadowski PD, Hyder BZ, Kanelis V, Davidson AR, Maxwell KL. HNH proteins are a widespread component of phage DNA packaging machines. Proc Natl Acad Sci USA 2014; 111: 6022–7.
29. Juhala RJ, Ford ME, Duda RL, Youlton A, Hatfull GF, Hendrix RW. Genomic sequences of bacteriophages HK97 and HK022: pervasive genetic mosaicism in the lambdoid bacteriophages. J Mol Biol 2000; 299: 27–51.
30. Yaginuma H, Kawai S, Tabata KV, Tomiyama K, Kakizuka A, Komatsuzaki T, Noji H, Imamura H. Diversity in ATP concentrations in a single bacterial cell population revealed by quantitative single-cell imaging. Sci Rep 2014; 4: 6522.
31. Feiss M, Rao VB. The bacteriophage DNA packaging machine. Adv Exp Med Biol 2012; 726: 489–509.
32. Quiles-Puchalt N, Carpena N, Alonso JC, Novick RP, Marina A, Penadés JR. Staphylococcal pathogenicity island DNA packaging system involving cos-site packaging and phage-encoded HNH endonucleases. Proc Natl Acad Sci USA 2014; 111: 6016–21.
33. Xu SY, Kuzin AP, Seetharaman J, Gutjahr A, Chan SH, Chen Y, Xiao R, Acton TB, Montelione GT, Tong L. Structure determination and biochemical characterization of a putative HNH endonuclease from Geobacter metallireducens GS-15. PLoS One 2013; 8: e72114.
34. Shen BW, Heiter DF, Chan SH, Wang H, Xu SY, Morgan RD, Wilson GG, Stoddard BL. Unusual target site disruption by the rare-cutting HNH restriction endonuclease PacI. Structure 2010; 18: 734–43.
35. Cue D, Feiss M. Termination of packaging of the bacteriophage lambda chromosome: cosQ is required for nicking the bottom strand of cosN. J Mol Biol 1998; 280: 11–29.
36. Xu SY, Boitano M, Clark TA, Vincze T, Fomenkov A, Kumar S, Too PH, Gonchar D, Degtyarev SK, Roberts RJ. Complete genome sequence analysis of Bacillus subtilis T30. Genome Announc 2015; 3: e00395–415.
37. Kelley LA, Sternberg MJ. Protein structure prediction on the Web: a case study using the Phyre server. Nat Protoc 2009; 4: 363–71.
38. Bujnicki JM, Radlinska M, Rychlewski L. Atomic model of the 5-methylcytosine-specific restriction enzyme McrA reveals an atypical zinc finger and structural similarity to betabetaalphaMe endonucleases. Mol Microbiol 2000; 37: 1280–1.
39. Han T, Yamada-Mabuchi M, Zhao G, Li L, Liu G, Ou H-Y, Deng Z, Zheng Y, He X. Recognition and cleavage of 5-methylcytosine DNA by bacterial SRA-HNH proteins. Nucleic Acids Res 2015; 43: 1147–59.
40. Zhang Y, Nelson M, Nietfeldt J, Xia Y, Burbank D, Ropp S, Van Etten JL. Chlorella virus NY-2A encodes at least 12 DNA endonuclease/methyltransferase genes. Virology 1998; 240: 366–75.
41. Chan SH, Zhu Z, Van Etten JL, Xu SY. Cloning of CviPII nicking and modification system from chlorella virus NYs-1 and application of Nt.CviPII in random DNA amplification. Nucleic Acids Res 2004; 32: 6187–99.
42. Chan SH, Zhu Z, Dunigan DD, Van Etten JL, Xu SY. Cloning of Nt.CviQII nicking endonuclease and its cognate methyltransferase: M.CviQII methylates AG sequences. Protein Expr Purif 2006; 49: 138–50.
43. Higgins LS, Besnier C, Kong H. The nicking endonuclease N.BstNBI is closely related to type IIs restriction endonucleases MlyI and PleI. Nucleic Acids Res 2001; 29: 2492–501.
44. Xu SY, Zhu Z, Zhang P, Chan SH, Samuelson JC, Xiao J, Ingalls D, Wilson GG. Discovery of natural nicking endonucleases Nb.BsrDI and Nb.BtsI and engineering of top-strand nicking variants from BsrDI and BtsI. Nucleic Acids Res 2007; 35: 4608–18.
45. Perevyazova TA, Rogulin EA, Zheleznaya LA, Matvienko NI. Cloning and sequencing of the gene of site-specific nickase N.BspD6I. Biochemistry (Mosc) 2003; 68: 984–7.
46. Kachalova GS, Rogulin EA, Yunusova AK, Artyukh RI, Perevyazova TA, Matvienko NI, Zheleznaya LA, Bartunik HD. Structural analysis of the heterodimeric type IIS restriction endonuclease R.BspD6I acting as a complex between a monomeric site-specific nickase and a catalytic subunit. J Mol Biol 2008; 384: 489–502.
47. Yunusova A, Rogulin E, Artyukh R, Zheleznaya L, Matvienko N. Nickase and a protein encoded by an open reading frame downstream from the nickase BspD6I gene form a restriction endonuclease complex. Biochemistry (Mosc) 2007; 71: 815–20.
48. Roberts RJ, Belfort M, Bestor T, Bhagwat AS, Bickle TA, Bitinaite J, Blumenthal RM, Degtyarev SKH, Dryden DT, Dybvig K, Firman K, Gromova ES, Gumport RI, Halford SE, Hattman S, Heitman J, Hornby DP, Janulaitis A, Jeltsch A, Josephsen J, Kiss A, Klaenhammer TR, Kobayashi I, Kong H, Krüger DH, Lacks S, Marinus MG, Miyahara M, Morgan RD, Murray NE, Nagaraja V, Piekarowicz A, Pingoud A, Raleigh E, Rao DN, Reich N, Repin VE, Selker EU, Shaw PC, Stein DC, Stoddard BL, Szybalski W, Trauner TA, Van Etten JL, Vitor JM, Wilson GG, Xu SY. A nomenclature for restriction enzymes, DNA methyltransferases, homing endonucleases and their genes. Nucleic Acids Res 2003; 31: 1805–12.
49. Zhu Z, Samuelson JC, Zhou J, Dore A, Xu SY. Engineering strand-specific DNA nicking enzymes from the type IIS restriction endonucleases BsaI, BsmBI, and BsmAI. J Mol Biol 2004; 337: 573–83.
50. Armalyte E, Bujnicki JM, Giedriene J, Gasiunas G, Kosiński J, Lubys A. Mva1269I: a monomeric type IIS restriction endonuclease from Micrococcus varians with two EcoRI- and FokI-like catalytic domains. J Biol Chem 2005; 280: 41584–94.
51. Too PH, Zhu Z, Chan SH, Xu SY. Engineering Nt.BtsCI and Nb.BtsCI nicking enzymes and applications in generating long overhangs. Nucleic Acids Res 2010; 38: 1294–303.
52. Janscak P, Sandmeier U, Szczelkun MD, Bickle TA. Subunit assembly and mode of DNA cleavage of the type III restriction endonucleases EcoP1I and EcoP15I. J Mol Biol 2001; 306: 417–31.
53. Gupta YK, Chan SH, Xu SY, Aggarwal AK. Structural basis of asymmetric DNA methylation and ATP-triggered long-range diffusion by EcoP15I. Nat Commun 2015; 6: 7363.

54. Xu Y, Lunnen KD, Kong H. Engineering a nicking endonuclease N.AlwI by domain swapping. Proc Natl Acad Sci USA 2001; 98: 12990–5.
55. Sanders KL, Catto LE, Bellamy SR, Halford SE. Targeting individual subunits of the FokI restriction endonuclease to specific DNA strands. Nucleic Acids Res 2009; 37: 2105–15.
56. Kostiuk G, Sasnauskas G, Tamulaitiene G, Siksnys V. Degenerate sequence recognition by the monomeric restriction enzyme: single mutation converts BcnI into a strand-specific nicking endonuclease. Nucleic Acids Res 2011; 39: 3744–53.
57. Sasnauskas G, Halford SE, Siksnys V. How the BfiI restriction enzyme uses one active site to cut two DNA strands. Proc Natl Acad Sci USA 2003; 100: 6410–5.
58. Lee K-Y, Lee K-Y, Kim J-H, Lee I-G, Lee S-H, Sim D-W, Won H-S, Lee B-J. Structure-based functional identification of Helicobacter pylori HP0268 as a nuclease with both DNA nicking and RNase activities. Nucleic Acids Res 2015; 43: 5194–207.
59. Murray IA, Stickel SK, Roberts RJ. Sequence-specific cleavage of RNA by Type II restriction enzymes. Nucleic Acids Res 2010; 38: 8257–68.
60. Matsuura M, Saldanha R, Ma H, Wank H, Yang J, Mohr G, Cavanagh S, Dunny GM, Belfort M, Lambowitz AM. A bacterial group II intron encoding reverse transcriptase, maturase, and DNA endonuclease activities: biochemical demonstration of maturase activity and insertion of new genetic information within the intron. Genes Dev 1997; 11: 2910–24.
61. Enyeart PJ, Mohr G, Ellington AD, Lambowitz AM. Biotechnological applications of mobile group II introns and their reverse transcriptases: gene targeting, RNA-seq, and non-coding RNA analysis. Mobile DNA 2014; 5: 2.
62. Cohen-Karni D, Xu D, Apone L, Fomenkov A, Sun Z, Davis PJ, Kinney SR, Yamada-Mabuchi M, Xu SY, Davis T, Pradhan S, Roberts RJ, Zheng Y. The MspJI family of modification-dependent restriction endonucleases for epigenetic studies. Proc Natl Acad Sci USA 2011; 108: 11040–45.
63. Bonocora RP, Shub DA. A likely pathway for formation of mobile group I introns. Curr Biol 2009; 19: 223–8.
64. Kong S, Liu X, Fu L, Yu X, An C. I-PfoP3I: a novel nicking HNH homing endonuclease encoded in the group I intron of the DNA polymerase gene in Phormidium foveolarum phage Pf-WMP3. PLoS One 2012; 7: e43738.
65. Metzger MJ, McConnell-Smith A, Stoddard BL, Miller AD. Single-strand nicks induce homologous recombination with less toxicity than double-strand breaks using an AAV vector template. Nucleic Acids Res 2011; 39: 926–35.
66. Metzger MJ, Stoddard BL, Monnat RJ, Jr. PARP-mediated repair, homologous recombination, and back-up non-homologous end joining-like repair of single-strand nicks. DNA Repair (Amst) 2013; 12: 529–34.
67. Katz SS, Gimble FS, Storici F. To nick or not to nick: comparison of I-SceI single- and double-strand break-induced recombination in yeast and human cells. PLoS One 2014; 9: e88840.
68. Xu S-y, Schildkraut I. Isolation of BamHI variants with reduced cleavage activities. J Biol Chem 1991; 266: 4425–9.
69. Roberts RJ, Vincze T, Posfai J, Macelis D. REBASE – a database for DNA restriction and modification: enzymes, genes and genomes. Nucleic Acids Res 2015; 43: D298–9.
70. Tevdoradze E, Farlow J, Kotorashvili A, Skhirtladze N, Antadze I, Gunia S, Balarjishvili N, Kvachadze L, Kutateladze M. Whole genome sequence comparison of ten diagnostic brucellaphages propagated on two Brucella abortus hosts. Virol J 2015; 12: 66.
71. Waugh DS, Sauer RT. Single amino acid substitutions uncouple the DNA binding and strand scission activities of Fok I endonuclease. Proc Natl Acad Sci USA 1993; 90: 9596–600.
72. Wah DA, Hirsch JA, Dorner LF, Schildkraut I, Aggarwal AK. Structure of the multimodular endonuclease FokI bound to DNA. Nature 1997; 388: 97–100.
73. Li L, Wu LP, Chandrasegaran S. Functional domains in FokI restriction endonuclease. Proc Natl Acad Sci USA 1992; 89: 4275–9.
74. Kim Y-G, Smith J, Durgesha M, Chandrasegaran S. Chimeric restriction enzyme: Gal4 fusion to FokI cleavage domain. Biol Chem 1998; 379: 489–95.
75. Bitinaite J, Wah DA, Aggarwal AK, Schildkraut I. FokI dimerization is required for DNA cleavage. Proc Natl Acad Sci USA 1998; 95: 10570–75.
76. Plagens A, Richter H, Charpentier E, Randau L. DNA and RNA interference mechanisms by CRISPR-Cas surveillance complexes. FEMS Microbiol Rev 2015; 39: 442–63.
77. Hsu PD, Scott DA, Weinstein JA, Ran FA, Konermann S, Agarwala V, Li Y, Fine EJ, Wu X, Shalem O, Cradick TJ, Marraffini, Bao G, Zhang F. DNA targeting specificity of RNA-guided Cas9 nucleases. Nat Biotechnol 2013; 31: 827–32.
78. Mali P, Aach J, Stranges PB, Esvelt KM, Moosburner M, Kosuri S, Yang L, Church Ran FA, Hsu PD, Lin CY, Gootenberg JS, Konermann S, Trevino AE, Scott DA, Inoue A, Matoba S, Zhang Y, Zhang FGM. CAS9 transcriptional activators for target specificity screening and paired nickases for cooperative genome engineering. Nat Biotechnol 2013; 31: 833–8.
79. Ran FA, Hsu PD, Lin CY, Gootenberg JS, Konermann S, Trevino AE, Scott DA, Inoue A, Matoba S, Zhang Y, Zhang F. Double nicking by RNA-guided CRISPR Cas9 for enhanced genome editing specificity. Cell 2013; 154: 1380–9.
80. Shen B, Zhang W, Zhang J, Zhou J, Wang J, Chen L, Wang L, Hodgkins A, Iyer V, XHuang Skarnes WC. Efficient genome modification by CRISPR-Cas9 nickase with minimal off-target effects. Nat Methods 2014; 11: 399–402.
81. Trevino AE, Zhang F. Genome editing using Cas9 nickases. Methods Enzymol 2014; 546: 161–74.
82. Xu T, Li Y, Shi Z, Hemme CL, Li Y, Zhu Y, Van Nostrand JD, He Z, Zhou J. Efficient genome editing in Clostridium cellulolyticum via CRISPR-Cas9 nickase. Appl Environ Microbiol 2015; 81: 4423–31.
83. Schiml S, Fauser F, Puchta H. The CRISPR/Cas system can be used as nuclease for in planta gene targeting and as paired nickases for directed mutagenesis in Arabidopsis resulting in heritable progeny. Plant J 2014; 80: 1139–50.
84. Fauser F, Schiml S, Puchta H. Both CRISPR/Cas-based nucleases and nickases can be used efficiently for genome engineering in Arabidopsis thaliana. Plant J 2014; 79: 348–59.
85. Ren X, Yang Z, Mao D, Chang Z, Qiao HH, Wang X, Sun J, Hu Q, Cui Y, Liu LP, Ji JY, Xu J, Ni JQ. Performance of the Cas9 nickase system in Drosophila melanogaster. G3 (Bethesda) 2014; 4: 1955–62.
86. Dow LE, Fisher J, O'Rourke KP, Muley A, Kastenhuber ER, Livshits G, Tschaharganeh DF, Socci ND, Lowe SW. Inducible in vivo genome editing with CRISPR-Cas9. Nat Biotechnol 2015; 33: 390–4.
87. Li K, Wang G, Andersen T, Zhou P, Pu WT. Optimization of genome engineering approaches with the CRISPR/Cas9 system. PLoS One 2014; 9: e105779.
88. Cho SW, Kim S, Kim Y, Kweon J, Kim HS, Bae S, Kim J-S. Analysis of off-target effects of CRISPR/Cas-derived RNA-guided endonucleases and nickases. Genome Res 2014; 24: 132–41.

89. Frock RL, Hu J, Meyers RM, Ho Y-J, Kii E, Alt FW. Genome-wide detection of DNA double-stranded breaks induced by engineered nucleases. Nat Biotechnol 2015; 33: 179–86.
90. Osborn MJ, Gabriel R, Webber BR, DeFeo AP, McElroy AN, Jarjour J, Starker CG, Wagner JE, Joung JK, Voytas DF, von Kalle C, Schmidt M, Blazar BR, Tolar J. Fanconi anemia gene editing by the CRISPR/Cas9 system. Hum Gene Ther 2015; 26: 114–26.
91. Byrne SM, Mali P, Church GM. Genome editing in human stem cells. Methods Enzymol 2014; 546: 119–38.
92. Wang JW, Wang A, Li K, Wang B, Jin S, Reiser M, Lockey RF. CRISPR/Cas9 nuclease cleavage combined with Gibson assembly for seamless cloning. Biotechniques 2014; 58: 161–70.
93. Price AA, Sampson TR, Ratner HK, Grakoui A, Weiss DS. Cas9-mediated targeting of viral RNA in eukaryotic cells. Proc Natl Acad Sci USA 2015; 112: 6164–9.
94. Ran FA, Cong L, Yan WX, Scott DA, Gootenberg JS, Kriz AJ, Zetsche B, Shalem O, Wu X, Makarova KS, Koonin EV, Sharp PA, Zhang F. In vivo genome editing using Staphylococcus aureus Cas9. Nature 2015; 520: 186–91.
95. Lam ET, Hastie A, Lin C, Ehrlich D, Das SK, Austin MD, Deshpande P, Cao H, Nagarajan N, Xiao M, Kwok P-Y. Genome mapping on nanochannel arrays for structural variation analysis and sequence assembly. Nat Biotechnol 2012; 30: 771–6.
96. Hastie AR, Dong L, Smith A, Finklestein J, Lam ET, Huo N, Cao H, Kwok P-Y, Deal KR, Dvorak J, Luo M-C, Gu Y, Xiao M. Rapid genome mapping in nanochannel arrays for highly complete and accurate de novo sequence assembly of the complex Aegilops tauschii genome. PLoS One 2013; 8: e55864.
97. Taylor JW, Schmidt W, Cosstick R, Okruszek A, Eckstein F. The use of phosphorothioate-modified DNA in restriction enzyme reactions to prepare nicked DNA. Nucleic Acids Res 1985; 13: 8749–64.
98. Walker GT, Fraiser MS, Schram JL, Little MC, Nadeau JG, Malinowski DP. Strand displacement amplification – an isothermal, in vitro DNA amplification technique. Nucleic Acids Res 1992; 20: 1691–6.
99. Walker GT, Little MC, Nadeau JG, Shank DD. Isothermal in vitro amplification of DNA by a restriction enzyme/DNA polymerase system. Proc Natl Acad Sci USA 1992; 89: 392–6.
100. Spargo CA, Fraiser MS, Van Cleve M, Wright DJ, Nycz CM, Spears PA, Walker GT. Detection of M. tuberculosis DNA using thermophilic strand displacement amplification. Mol Cell Probes 1996; 10: 247–56.
101. Van Ness J, Van Ness LK, Galas DJ. Isothermal reactions for the amplification of oligonucleotides. Proc Natl Acad Sci USA 2003; 100: 4504–9.
102. Qian J, Ferguson TM, Shinde DN, Ramírez-Borrero AJ, Hintze A, Adami C, Niemz A. Sequence dependence of isothermal DNA amplification via EXPAR. Nucleic Acids Res 2012; 40: e87.
103. Antipova VN, Zheleznaya LA, Zyrina NV. Ab initio DNA synthesis by Bst polymerase in the presence of nicking endonucleases Nt.AlwI, Nb.BbvCI, and Nb.BsmI. FEMS Microbiol Lett 2014; 357: 144–50.
104. Dong H, Meng X, Dai W, Cao Y, Lu H, Zhou S, Zhang X. Highly sensitive and selective microRNA detection based on DNA-bio-bar-code and enzyme-assisted strand cycle exponential signal amplification. Anal Chem 2015; 87: 4334–40.
105. Miao P, Han K, Wang B, Luo G, Wang P, Chen M, Tang Y. Electrochemical detection of aqueous Ag^+ based on Ag^+-assisted ligation reaction. Sci Rep 2015; 5: 9161.
106. Du R, Li S, Zhang X. A modified plasmid vector pCMV-3Tag-LIC for rapid, reliable, ligation-independent cloning of polymerase chain reaction products. Anal Biochem 2011; 408: 357–59.
107. Oster CJ, Phillips GJ. Vectors for ligation-independent construction of lacZ gene fusions and cloning of PCR products using a nicking endonuclease. Plasmid 2011; 66: 180–5.
108. Bitinaite J, Rubino M, Varma KH, Schildkraut I, Vaisvila R, Vaiskunaite R. USER friendly DNA engineering and cloning method by uracil excision. Nucleic Acids Res 2007; 35: 1992–2002.
109. Chen Y-J, Dalchau N, Srinivas N, Phillips A, Cardelli L, Soloveichik D, Seelig G. Programmable chemical controllers made from DNA. Nat Nanotechnol 2013; 8: 755–62.
110. Miyamoto T, Razavi S, DeRose R, Inoue T. Synthesizing biomolecule-based Boolean logic gates. ACS Synth Biol 2013; 2: 72–82.
111. Chan SH, Stoddard BL, Xu SY. Natural and engineered nicking endonucleases – from cleavage mechanism to engineering of strand-specificity. Nucleic Acids Res 2011; 39: 1–18.
112. Yan L, Zhou J, Zheng Y, Gamson AS, Roembke BT, Nakayama S, Sintim HO. Isothermal amplified detection of DNA and RNA. Mol Biosyst 2014; 10: 970–1003.
113. Pei J, Kim BH, Grishin NV. PROMALS3D: a tool for multiple protein sequence and structure alignments. Nucleic Acids Res 2008; 36: 2295–300.

Supplemental Material: The online version of this article (DOI: 10.1515/bmc-2015-0016) offers supplementary material, available to authorized users.